

## Every zircon deserves a date: selection bias in detrital geochronology

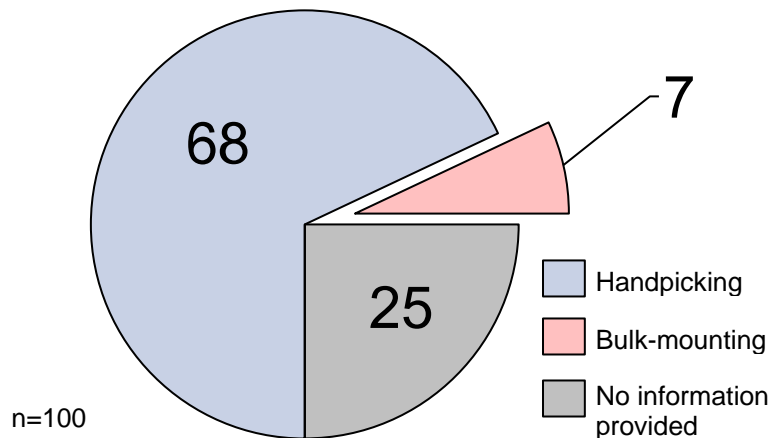
Maximilian Dröllner<sup>1,\*</sup>, Milo Barham<sup>1</sup>, Christopher L. Kirkland<sup>1</sup>, and Bryant Ware<sup>2</sup>

<sup>1</sup> *Timescales of Mineral Systems, School of Earth and Planetary Sciences, Curtin University, GPO Box U1987, Perth, WA 6845, Australia*

<sup>2</sup> *John de Laeter Centre for Isotope Research, Curtin University, GPO Box U1987, Perth, WA 6845, Australia*

\*Email: [maximilian.droellner@postgrad.curtin.edu.au](mailto:maximilian.droellner@postgrad.curtin.edu.au)

### Supplementary Figure S1 and Supplementary Material S1 (*Detailed methods*)



**Supplementary Figure S1.** *Compilation of mounting techniques in recent publications (n=100). Studies using handpicking are significantly more numerous than those employing bulk-mounting (68 handpicking versus 7 bulk-mounting). The first 100 publications presenting new detrital zircon geochronology data listed in Google Scholar using “detrital zircon geochronology” as the search term from 2020 have been manually evaluated regarding the applied mounting technique.*

## **U-Pb Geochronology**

The 53-1000  $\mu\text{m}$  grain size fraction underwent heavy liquid separation at  $2.96 \text{ g/cm}^3$  and isodynamic magnetic separation resulting in a zircon-dominated mineral separate. Coning and quartering was performed to maintain representativeness of the zircon separate. One aliquot was used for handpicking, another for bulk mounting. Handpicking was performed using a binocular stereo microscope and a needle to transfer zircon grains from a glass petri dish onto sticky tape. The handpicking operator was attempting to sample a representative zircon population and has no diagnosed colour vision deficiency. Bulk mounting was done on the same mount, ensuring consistency of the resin medium for imaging. Zircon grains were embedded in epoxy resin in a 25 mm diameter mount and polished to maximise exposure of the grains mounted. To avoid mixtures of age components cathodoluminescence imaging using a Tescan Clara FESEM (Czech Republic) was performed before analysis. Zircon grains were analysed by laser ablation-inductively coupled plasma-mass spectrometry (LA-ICP-MS) at Curtin University's John de Laeter Centre (Perth, Australia). Sample preparation (including handpicking) and geochronological analysis (including spot placement) were conducted by two independent operators. The majority of both the handpicked and bulk-mounted zircon grains (approximately 80 % and 70 %, respectively) were analysed. Remaining grains usually did not allow spot placement within single growth domains, or avoiding fractures and/or inclusions. Analysing the majority of zircon grains and having spot placement undertaken by the same operator for handpicked and bulk-mounted grains precludes analytical bias between populations related to operator selection.

An excimer laser (RESolution LR 193 nm ArF) was used with a laser fluence of  $4.5 \text{ J cm}^{-2}$  and repetition rate of 5 Hz for  $\sim 30 \text{ s}$  of analysis time and 20 s of background capture. Two cleaning pulses preceded all analyses. The sample cell was flushed by ultrahigh purity He ( $341 \text{ mL min}^{-1}$ ) and  $\text{N}_2$  ( $3.6 \text{ mL min}^{-1}$ ) and ablations were  $30.0 \mu\text{m}$  circular spots.

**Supplementary Material S1:** Every zircon deserves a date: selection bias in detrital geochronology

The U-Pb isotope analyses were acquired using a sector field ICP-MS ELEMENT XR (ThermoScientific). Prior to each analytical session, a line scan ablation of the NIST612 glass was used to tune instrument adjusting settings to obtain a high intensity, stable signal, and low oxide rates ( $^{232}\text{Th}^{16}\text{O}/^{232}\text{Th}$ , 0.05 %). Measurements of masses  $^{202}\text{Hg}$ ,  $^{204}\text{Pb}$ ,  $^{206}\text{Pb}$ ,  $^{207}\text{Pb}$ ,  $^{232}\text{Th}$ , and  $^{238}\text{U}$  were performed in low resolution mode using electrostatic scanning (e-scan, i.e., peak jumping) from a set magnet mass at  $^{202}\text{Hg}$ . In the low-resolution mode of a magnetic sector field ICP-MS large, flat peak tops and fast electronic scanning from a locked magnet position enable an improved measurement of the peak signal intensity by allowing multiple sampling of the peak tops across the peak. Time resolved intensity data were acquired in a pulse-counting detection mode for mass  $^{202}\text{Hg}$  and using the ELEMENT XR's triple detection mode for the remaining masses,  $^{204}\text{Pb}$ ,  $^{206}\text{Pb}$ ,  $^{207}\text{Pb}$ ,  $^{232}\text{Th}$ , and  $^{238}\text{U}$ . Due to low abundance, and because a more precise  $^{207}\text{Pb}/^{235}\text{U}$  ratio can be calculated from the  $^{207}\text{Pb}/^{206}\text{Pb}$  and  $^{206}\text{Pb}/^{238}\text{U}$  ratios and the natural abundance of  $^{238}\text{U}/^{235}\text{U}$ ,  $^{235}\text{U}$  was not analysed. Interference of  $^{204}\text{Hg}$  from the carrier gas on  $^{204}\text{Pb}$  was quantified by monitoring  $^{202}\text{Hg}$  (the most abundant Hg isotope and contains no major interferences). As total  $^{204}\text{Pb}$  counts were low for concordant analyses, no common Pb correction is deemed necessary. Operating parameters for both the ICPMS and laser instruments can be found in Table S1 (found in the Supplementary Material S2).

Data reduction was performed using *iolite4* (Paton *et al.* 2011). 91500 zircon (Wiedenbeck *et al.* 1995) was used as the primary reference material. Secondary reference materials GJ1 (Jackson *et al.* 2004), and Plešovice (Sláma *et al.* 2008) were measured as unknowns at regular intervals to allow confirmation of precision and accuracy. Results of reference materials are listed in Table S2. External reproducibility was obtained from the GJ1 reference. Ages are quoted at  $2\sigma$  absolute uncertainty.

## **Supplementary Material S1: Every zircon deserves a date: selection bias in detrital geochronology**

To avoid arbitrary discordance filters, we only use concordant ages as defined where the two-sigma error ellipse intercepts the Concordia curve. Additionally, to avoid changing between different ratios for age calculation, and to make optimum use of both U/Pb and Pb/Pb ratios, Concordia ages are used in all calculations. Statistics for U-Pb ages were performed using DZstats (Saylor & Sundell, 2016). Statistics for grain shape and colour analyses were performed using PAST4.03 (Hammer *et al.* 2001). Zircon age spectra are visualized as kernel density estimates and cumulative age distributions using the IsoplotR software (Vermeesch, 2018).

### **Calculation of colour bias**

We test a partial correction calculation based on the discrepancy of colour (here:  $\Sigma$  Colour [%]) between bulk-mounted and handpicked population. The difference in colour populations can be visualized and quantified using histogram binning of  $\Sigma$  Colour (Fig. 7a).

Grains with  $>18\%$   $\Sigma$  Colour are overrepresented in the handpicked population while those with  $<16\%$   $\Sigma$  Colour are underrepresented. We calculated the ratio of the fractions ‘bulk-mounted grains  $>18\%$   $\Sigma$  Colour’ over ‘handpicked grains  $>18\%$   $\Sigma$  Colour’ to determine the degree to which handpicked grains of this colour need to be reduced. A ratio of 0.12 suggests reducing components of age modes  $>18\%$   $\Sigma$  Colour by 88%. Similarly, we perform a relative addition by calculating the ratio of the fractions ‘bulk-mounted grains  $<16\%$   $\Sigma$  Colour’ over ‘handpicked grains  $<16\%$   $\Sigma$  Colour’. A value of 1.48 supports increasing the components  $<16\%$   $\Sigma$  Colour of every age mode by 48%.

For instance, age mode LC.2 has 0 counts  $>18\%$   $\Sigma$  Colour and 10 counts  $<16\%$   $\Sigma$  Colour resulting in subtraction of 0 counts and addition of 5 counts, respectively. Thus, age mode LC.2 increases from 11 to 16 counts. Adjustment of the new age population was done by randomly adding pre-existing ages or discarding ages of the different age modes (bootstrapping).

## **Supplementary Material S1: Every zircon deserves a date: selection bias in detrital geochronology**

In total, the overrepresented age modes AFO.1, AFO.2, and YG reduce their relative proportions of the total population while the underrepresented age mode LC.2 increases its proportion. Calculated metrics of inter-sample comparison using the new age distribution show higher similarity. Supporting documentation of the calculation is provided Table S7 and visualized in Figure 7a,b.

### **References**

**Hammer, Ø., Harper, D. A. T. & Ryan, P. D.** (2001) PAST: Paleontological statistics software package for education and data analysis. *Palaeontologia electronica* **4**, 9.

**Jackson, S. E., Pearson, N. J., Griffin, W. L. & Belousova, E. A.** (2004) The application of laser ablation-inductively coupled plasma-mass spectrometry to in situ U–Pb zircon geochronology. *Chemical Geology* **211**, 47–69.

**Paton, C., Hellstrom, J., Paul, B., Woodhead, J. & Hergt, J.** (2011) Iolite: Freeware for the visualisation and processing of mass spectrometric data. *Journal of Analytical Atomic Spectrometry* **26**, 2508.

**Saylor, J. E. & Sundell, K. E.** (2016) Quantifying comparison of large detrital geochronology data sets. *Geosphere* **12**, 203–20.

**Sláma, J., Košler, J., Condon, D. J., Crowley, J. L., Gerdes, A., Hanchar, J. M., Horstwood, M. S., Morris, G. A., Nasdala, L., Norberg, N., Schaltegger, U., Schoene, B., Tubrett, M. N. & Whitehouse, M. J.** (2008) Plešovice zircon — A new natural reference material for U–Pb and Hf isotopic microanalysis. *Chemical Geology* **249**, 1–35.

**Vermeesch, P.** (2018) IsoplotR: A free and open toolbox for geochronology. *Geoscience Frontiers* **9**, 1479–93.

**Wiedenbeck, M., Allé, P., Corfu, F., Griffin, W. L., Meier, M., Oberli, F. & Quadt, A. von** (1995) Three Natural Zircon Standards for U-Th-Pb, Lu-Hf, Trace Element and REE Analyses. *Geostandards and Geoanalytical Research* **19**, 1–23.